Real-time monitoring of the dissolution of silver nanoparticles by using a solid-contact Ag^+-selective electrode

Yin, Tanji; Han, Tingting; Li, Changbai; Qin, Wei; Bobacka, Johan

Published in:
Analytica Chimica Acta

DOI:
10.1016/j.aca.2019.12.022

Published: 08/03/2020

Document Version
Accepted author manuscript

Real-time monitoring of the dissolution of silver nanoparticles by using a solid-contact Ag^+-selective electrode

Tanji Yin [a, b, c], Tingting Han [b], Changbai Li [b], Wei Qin [a, c], Johan Bobacka [b]*

[a] *CAS Key Laboratory of Coastal Environmental Processes and Ecological Remediation, Yantai Institute of Coastal Zone Research (YIC), Chinese Academy of Sciences (CAS); Shandong Key Laboratory of Coastal Environmental Processes, YICCAS, Yantai, Shandong 264003, P. R. China*

[b] *Laboratory of Molecular Science and Engineering, Johan Gadolin Process Chemistry Centre, Åbo Akademi University, Biskopsgatan 8, FIN-20500 Turku/Åbo, Finland*

c Laboratory for Marine Biology and Biotechnology, Qingdao National Laboratory for Marine Science and Technology, Qingdao 266200, P. R. China

*Corresponding author. *E-mail address*: johan.bobacka@abo.fi

Abstract

The dissolution kinetics of silver nanoparticles (Ag NPs) to Ag^+ ions is a critical factor determining the toxicity of silver nanoparticles. In this work, a solid-contact Ag^+-selective electrode (Ag^+-ISE) is fabricated and used to monitor the dissolution of Ag NPs. Ordered mesoporous carbon is compared with disordered mesoporous carbon as the solid-contact material for the Ag^+-ISE. The ordered mesoporous carbon based solid-contact Ag^+-ISE shows a linear potential response in the range of 1.0×10^{-6}-1.0×10^{-3} M $AgNO_3$ with the slope of 55.6 ± 0.8 mV/dec (n = 7) and the detection limit of $10^{-6.8}$ M. The solid-contact Ag^+-ISE is used to monitor the concentration changes of Ag^+ during spontaneous dissolution of Ag NPs in deionized water, and the dissolution kinetics of Ag NPs is consistent with that obtained by inductively coupled plasma-mass spectrometry (ICP-MS). Stimulated dissolution of Ag NPs induced by addition of H_2O_2 to the Ag NP solution is also investigated by the proposed solid-contact Ag^+-ISE. This work provides a fast tool for charactering the dissolution of Ag NPs to Ag^+ in real time, which is important for studying the toxicology of nanoparticles.

Keywords: Solid-contact Ag^+-selective electrode; Mesoporous carbon; Spontaneous dissolution; Stimulated dissolution; Ag^+

1. Introduction

Nanotoxicology research is gaining more and more attention due to the increased risk of exposure and release of nanomaterials in the environment as a result of mass production and extensive use of various nanoparticles [1]. Silver nanoparticles (Ag NPs), being one of the most popular nanomaterials, are widely used in commercial products, due to their unique antibacterial, antiviral and antifungal properties [2]. In fact, the toxicity of Ag NPs is hard to be ignored, because Ag NPs are easily released into the environment during the application, handling and disposal of these commercial products. In recent years, extensive research about the toxicity of Ag NPs has been carried out [3-5], and the free Ag^+ ions released from Ag NPs are found to determine part of the toxicity [6, 7]. Therefore, dynamic monitoring of the dissolution of Ag NPs to Ag^+ is essential in order to understand how the toxicity of nanoparticles affect on organisms and ecosystems.

Atomic absorption spectrometry (AAS) and inductive coupled plasma mass spectrometry (ICP-MS) are two commonly used techniques for detection of the amount of Ag^+ released from Ag NPs [8-10]. These atomic spectroscopic methods show high selectivity and sensitivity. However, these methods not only need expensive instruments and complex operation, but also cannot provide real-time assessment of the kinetics of Ag NPs dissolution. Moreover, these methods are not selective to Ag^+ ions in the presence of AgNPs.

Ion-selective electrodes (ISEs) is a promising tool for studying the kinetics of Ag NPs dissolution and differentiating free Ag^+ and complexed Ag^+ [11-14]. ISEs also

show other unique characteristics, such as small size, ease of operation, portability and low cost. Among these ISEs, the commercial solid-state Ag_2S-based ISEs are frequently used to monitoring the dissolution of Ag NPs. However, the analytical performance of such electrodes is easily influenced by interferents, which would strongly adsorb on the surface of the solid-state Ag_2S electrodes [15]. In addition, most of the reported Ag^+-ISEs contain an inner filling solution [15-17], which may need frequent maintenance that prevents long-term monitoring of the dissolution of Ag NPs.

Solid-contact ISEs are recognized as the next generation of ISEs [18, 19], due to the straightforward fabrication, and convenient usability and storage. Solid-contact ISEs have been constructed using various solid-contact materials, including conducting polymers [19] and several kinds of porous materials such as three-dimensional ordered macroporous carbon [20, 21], colloid-imprinted mesoporous carbon [22], three-dimensional porous graphene-mesoporous platinum nanoparticle composite [23] and nanoporous gold [24]. However, as far as we know, there are few reports about monitoring the dissolution of Ag NPs by using solid-contact Ag^+-ISEs.

In this work, solid-contact Ag^+-selective electrodes based on ordered and disordered mesoporous carbon materials as solid contact are developed. The influence of the morphology of mesoporous carbon materials on the electrochemical properties and the potentiometric performance of the proposed Ag^+-ISEs is investigated. The ordered mesoporous carbon-based solid contact is used to fabricate stable and robust solid-contact Ag^+-ISE to monitor the spontaneous and stimulated dissolution of Ag NPs in water.

2. Experimental

2.1 Reagents and materials

Ag^+ ionophore (*o*-xylylenebis(*N, N*-diisobutyldithiocarbamate)), potassium tetrakis[3,5-bis(trifluoromethyl)phenyl]borate (KTFPB), bis(2-ethylhexyl) sebacate (DOS), high molecular weight poly(vinyl chloride) (PVC), and tetrahydrofuran (THF) were purchased from Sigma-Aldrich. Ordered mesoporous carbon (OMC) with BET surface area ≥ 900 m^2/g and average pore diameter of 3.8-4 nm, and disordered mesoporous carbon (DOMC) with Brunauer-Emmett-Teller (BET) surface area of about 600 m^2/g and average pore diameter of 50 nm were obtained from Nanjing XFNANO Materials Tech Co.,Ltd. All other chemicals were of analytical reagent grade. Deionized water (18.2 MΩ cm specific resistance) obtained with a Pall Cascada laboratory water system was used throughout.

2.2 Synthesis of Ag nanoparticles

Ag NPs stabilized with citrate were synthesized with some modifications according to the literature [25]. Briefly, 0.86 ml of 58.8 mM $AgNO_3$ and 4.4 ml of 34 mM sodium citrate were added to 200 ml of boiling deionized water under stirring, and then 1 ml of freshly prepared 0.1 M $NaBH_4$ was drop-wise added to the above solution. The final solution was kept boiling for 30 min, and finally allowed to cool down to room temperature. The obtained Ag NPs were purified with regenerated cellulose (MWCO 50kD) centrifuge filter units at 5000 r/min for 5 min to remove the excess reagents, and then collected after washing three times with deionized water.

2.3 Preparation of the solid-contact Ag^+-ISEs

The GC disk electrodes (3 mm in diameter) were successively polished with abrasive papers of different coarseness, diamond pastes with particle diameters of 15, 9, 3 and 1 μm, and finally with 0.3 and 0.05 μm Al_2O_3 paste. After being ultrasonically cleaned and rinsed with deionized water, the polished electrodes were used to prepare the mesoporous carbon nanomaterials-based solid contact. The solid-contact suspensions were prepared by ultrasonicating 6 mg of the ordered and disordered mesoporous carbon materials in 2 ml of freshly distilled THF for 30 min. An amount of 60 μl of the prepared solid-contact suspensions were drop cast on the GC electrodes in order to homogeneously coat the surface of the GC electrodes, and then left to dry at room temperature for further use.

The Ag^+-selective membrane contains 0.77 wt% Ag^+ ionophore, 0.44% KTFPB, 32.93 wt% PVC and 65.86 wt% DOS. The membrane cocktail was prepared by dissolving 360 mg of membrane components in 4 ml of THF and stirred for at least 2 h to obtain a homogeneous solution. Then, 90 μl of the membrane cocktail was separately drop cast on the above ordered and disordered mesoporous carbon modified GC electrodes to prepare the proposed solid-contact Ag^+-ISEs. After being dried at room temperature, the electrodes, which were denoted as GC/OMC/Ag^+-ISE and GC/DOMC/Ag^+-ISE, were conditioned in 1.0×10^{-4} M $AgNO_3$ for 2 days. For comparison, the coated-disk Ag^+-ISE (GC/Ag^+-ISE) was also prepared by directly dropping the Ag^+-selective membrane cocktail on the bare GC electrode.

2.4 Apparatus and measurements

Ag NPs were characterized by transmission electron microscopy (TEM, JEM-1400, JEOL, Japan), UV-visible spectroscopy (Nanodrop 2000C, Thermo Scientific, DE) and particle size distribution measurements (Zetasizer Nano ZS90, Malvern, UK). For investigating the dissolution of Ag NPs, the released Ag^+ in the supernatants was collected at 1, 2, 4, 6 and 8 h by using centrifugal filter units at 7000 r/min for 8 min, and characterized by inductively coupled plasma-mass spectrometry (ICP-MS), respectively.

Potentiometric measurements were carried out by using a 16-channel potentiometer (EMF 16, Lawson Labs, USA) at room temperature with a double junction Ag/AgCl (3 M KCl)/1.0 M LiOAc electrode as a reference electrode in the galvanic cell: Ag|AgCl(3 M KCl)|1.0 M LiOAc|sample solution|Ag^+-selective membrane| mesoporous carbon|GC electrode. The ion activities and liquid junction potentials were calculated by the Debye-Hückel and Henderson equations, respectively. To monitor the spontaneous dissolution of Ag NPs, the ordered mesoporous carbon-based solid-contact Ag^+-ISE was immersed in deionized water. Then a certain volume of the prepared Ag NP solution was added under continuous recording of the potential of the solid-contact Ag^+-ISE. To monitor the stimulated dissolution of Ag NPs, 0.1 M H_2O_2 was added in a solution containing Ag NPs to release Ag^+.

Cyclic voltammetry (CV) and electrochemical impedance spectroscopy (EIS) were performed by using the Autolab potentiostat/Galvanostat equipped with a frequency response analyzer (AUT20. FRA2-AUTOLAB, Eco Chemie, B.V., The Netherlands)

with a three-electrode system in 0.1 M KNO_3, where the mesoporous carbon modified GC electrode was used as a working electrode, an Ag/AgCl (3 M KCl) as reference electrode and a GC rod as auxiliary electrode. Multi-chronopotentiometry was carried out on the mesoporous carbon-based solid-contact Ag^+-ISEs in 0.1 M KNO_3 by applying constant currents of ±1 nA for 60 s, respectively.

3. Results and discussion

3.1 Electrochemical behavior of the ordered and disordered mesoporous carbon based solid contacts

The morphologies of the mesoporous carbon materials, which is directly related to the pore size distribution, shapes and volume of void spaces in porous materials [26], may affect the electrochemical behavior of the mesoporous carbon-based solid contacts. In this work, both ordered and disordered mesoporous carbon materials are chosen as candidates to be as solid contacts for preparing solid-contact Ag^+-ISEs. The electrochemical behavior of the mesoporous carbon materials with different morphologies (GC/OMC and GC/DOMC) are compared with CV and EIS. As shown in Fig. 1, the bare GC electrode shows a very small capacitive current, while the GC/OMC and GC/DOMC electrodes display large capacitive currents. Moreover, the capacitive current for the GC/OMC electrode is found to be higher than that of the GC/DOMC electrode, which may be due to the fact that the ordered mesoporous carbon shows a larger BET surface area and a smaller pore diameter than those for the disordered mesoporous carbon. Additionally, according to the equation [27], C =

$Q_m/\Delta V$, where Q_m is the specific voltammetric charge integrated from the cyclic voltammetric curve, and ΔV is the potential scanning range, the specific capacitance of the bare GC, GC/DOMC and GC/OMC electrodes are estimated to be 0.005, 4.0 and 6.6 mF, respectively. These results demonstrate that the GC/OMC electrode shows a significantly higher double layer capacitance than those for the bare and GC/DOMC electrodes, i.e. the electrochemical behavior of the solid contacts in 0.1 M KNO_3 is influenced by the different morphology characteristics of mesoporous carbon materials.

EIS is also performed to compare the interfacial characteristics for the ordered and disordered mesoporous carbon modified GC electrodes. As shown in Fig. 2, the impedance spectra for the GC/OMC and GC/DOMC electrodes show absence of semicircles in the high-frequency region, indicating that both electrodes exhibit high electronic conductivity and fast ion transfer. Moreover, the GC/OMC electrode displays a closer to 90º capacitive line than that for the GC/DOMC electrode in the low-frequency region, indicating that the ordered mesoporous carbon modified GC electrode shows a more ideal capacitive characteristic than the disordered mesoporous carbon modified electrode. Additionally, the double layer capacitance for the GC/OMC electrode (10.7 mF) is found to be larger than that for the GC/DOMC electrode (8.5 mF), according to the equation, $C = -1/(2\pi fZ'')$， where f is the frequency and Z'' is the imaginary part of the impedance. This phenomenon is consistent with that for the cyclic voltammograms, although the values are slightly different between the two methods, as demonstrated by Bühlmann's group [22]. These results indicate that the ordered mesoporous carbon is more suitable as solid contact than disordered mesoporous

carbon, since a sufficiently high bulk capacitance for the solid contact is a prerequisite for constructing a stable and robust solid-contact ISE [28].

3.2 Characterization of the mesoporous carbon-based solid-contact Ag^+-ISEs

In order to further study the influence of the morphologies of the mesoporous carbon materials on the potentiometric performance, the solid-contact Ag^+-ISEs were prepared by using the ordered and disordered mesoporous carbon materials as solid contacts, respectively. Multi-chronopotentiometry was used to investigate the potential stability of the proposed electrodes, instead of single chronopotentiometry [28]. As shown in Fig. 3, the chronopotentiograms of the ordered and disordered mesoporous carbon-based solid-contact Ag^+-ISEs show the same shape characteristics as that for the coated-disk Ag^+-ISE. That is, two main features, including a potential jump when changing the direction of the current and a slow potential drift as the time increases, are observed. However, the numerical values of the potential drift are significantly different for the GC/Ag^+-ISE (190 ± 5 μV/s, n = 5), GC/OMC/Ag^+-ISE (28 ± 4 μV/s, n = 5) and GC/DOMC/Ag^+-ISE (29 ± 2 μV/s, n = 5), according to the ratio $\Delta E/\Delta t$ obtained by the potential changes during the time intervals = 30-60 and 90-120 s. As expected, the presence of the mesoporous carbon materials between the GC electrode and Ag^+-selective membrane can effectively improve the potential stability of the solid-contact Ag^+-ISEs by facilitating interfacial ion- and electron-transfer processes at the GC/solid contact and solid contact/ion-selective membrane interfaces, respectively. However, contrary to predictions from CV (Fig. 1) and EIS (Fig. 2), the potential drift for the ordered mesoporous carbon-based solid-contact Ag^+-ISE is found to be only slightly

smaller than that for the disordered mesoporous carbon-based electrode. This result indicates that the capacitance of OMC and DOMC are only partly accessible after coverage with the ion-selective membrane. Similar features have been reported for solid contacts based on poly(3,4-ethylenedioxythiophene) (PEDOT) [28]. Here, the ordered mesoporous carbon-based solid-contact Ag^+-ISE was selected to monitor the dissolution of Ag NPs.

In this work, the compound, *o*-xylylenebis(*N, N*-diisobutyldithiocarbamate), was chosen as Ag^+ ionophore, since it shows very high selectivity toward Ag^+ [29-31], as compared with other Ag^+ ionophores [32, 33]. This means that the proposed ionophore-based solid-contact Ag^+-ISE may be useful for monitoring the dissolution of Ag NPs in complex background solutions. The potentiometric performance of the ordered mesoporous carbon-based solid-contact Ag^+-ISE was investigated by successively increasing Ag^+ activities. As shown in Fig. 4, the proposed electrode shows a stable linear potentiometric response in the range of 1.0×10^{-6} - 1.0×10^{-3} M with a slope of 55.6 ± 0.8 mV/dec (n = 7), and the detection limit calculated as the intersection of the two slope lines is $10^{-6.8}$ M. Additionally, in order to monitor the dissolution of Ag NPs in real time, the long-term potential stability of the proposed Ag^+-ISE needs to be investigated. As shown in Fig. 5, the potential responses of the GC/OMC/Ag^+-ISE are continuously measured under zero current condition for 16 h in 1.0×10^{-4} and 1.0×10^{-5} M $AgNO_3$, and the potential drifts are estimated to be 0.16 ± 0.09 and 0.21 ± 0.08 mV/h (n = 3) in 1.0×10^{-4} and 1.0×10^{-5} M $AgNO_3$, respectively. These drift values are sufficiently small when compared to the potential change caused by the released Ag^+

from Ag NPs to allow real-time monitoring of Ag^{+}.

3.3 Characterization of silver nanoparticles

Home-made citrate-capped Ag NPs were chosen as a model for studying the dissolution of Ag NPs, since citrate is commonly used as Ag NPs capping agents. As shown in Fig. 6, the prepared Ag NPs show good spherical distribution, and the average diameter is estimated to be about 8.9 ± 1.8 nm. Additionally, the prepared Ag NP solution was also characterized by UV-visible spectroscopy. As shown in Fig. 6c, the typical absorbance peak is observed at about 392.5 nm. According to the literature [34], the concentration of the prepared Ag NP solution can be estimated by using the extinction coefficient of 5.56 M^{-1} cm^{-1}. The unit of the concentration of Ag NPs is expressed as μg/ml, which is obtained by calculating the number of atoms per nanoparticle and converting atoms to mass using the atomic weight of Ag [7]. The numbers of atoms per nanoparticle (U) are calculated by the following equation: $U = (2/3)\pi(D/a)^3$ [35]. Where, D is the average nanoparticle diameter (8.9 nm), and a is the edge length of a Ag unit cell (4.0857 Å). In this work, 0.3 μg/ml Ag NP solution was selected for investigating the dissolution of Ag NPs, which is within the concentration range of 0.01-18 μg/ml Ag NPs that is released into the environment through wastewater [36, 37].

3.4 Investigation of the dissolution of Ag NPs

Both the spontaneous dissolution and the stimulated dissolution of Ag NPs were

monitored by using the proposed mesoporous carbon-based solid-contact Ag^+-ISE in deionized water. Before the dissolution measurements, the potentiometric performance of the proposed Ag^+-ISE was measured and calibrated. For the spontaneous dissolution, Ag NPs were added to the deionized water with slow-speed stirring, and the proposed solid-contact Ag^+-ISE was used to monitoring the changes of the concentrations of Ag^+ released from Ag NPs in real time for 8 h. Meanwhile, the spontaneous dissolution of Ag NPs was also measured with ICP-MS by collecting the supernatants of the Ag NP solution at discrete time points, including 1, 2, 4, 6 and 8 h. As shown in Fig. 7a, the potential response of the electrode shows three main features: a potential equilibration of the electrode in deionized water, a fast positive potential change due to the residual Ag^+ in the Ag NP solution, and a slowly increasing potential response due to the release of Ag^+ from Ag NPs. According to the calibration curve (Fig. 4), the real-time concentration changes of Ag^+ after the addition of Ag NPs in deionized water are calculated and shown in Fig. 7b. It can be seen that the concentration of the released Ag^+ at discrete points obtained by the proposed Ag^+-ISE and ICP-MS show no significant differences for the spontaneous dissolution of Ag NPs, while the proposed Ag^+-ISE provides real-time kinetics assessment for the dissolution of Ag NPs as compared with ICP-MS.

Ag NPs may undergo different chemical and morphological transformations, once they are released into the environment. In this work, H_2O_2 is selected as a model to monitor the stimulated dissolution of Ag NPs. As shown in Fig. 8a, there is a significant positive potential change caused by the residual Ag^+ upon the addition of Ag NPs,

compared to the case of spontaneous dissolution of Ag NPs in Fig. 7a. This is presumably due to the faster stirring rate used in Fig. 8 than in Fig. 7. Moreover, another positive potential change is also observed upon the addition of H_2O_2, due to the fact that H_2O_2 oxidizes Ag NPs to free Ag^+. Additionally, it can be seen that the stimulated dissolution rate of Ag NPs, which is related to the concentrations of H_2O_2, is observed to be faster than the spontaneous dissolution rate. In order to confirm the stimulated dissolution process of Ag NPs to Ag^+, 0.1 M NaCl was added in the Ag NP solution. As shown in Fig. 8, the potential of the proposed solid-contact Ag^+-ISEs is found to drop instantaneously upon the addition of 0.1 M NaCl, indicating that the concentration of the released Ag^+ decreases due to the formation and precipitation of AgCl. These phenomena indicate that the proposed solid-contact Ag^+-ISE shows a fast and reversible response to the concentration changes of free Ag^+ released from Ag NPs.

4. Conclusions

This work develops a solid-contact Ag^+-ISE based on mesoporous carbon as solid contact and applies it to characterize the dissolution of Ag NPs in water. The influence of the morphologies of the solid contact on the electrochemical behavior and the potentiometric stability of the solid-contact Ag^+-ISEs are investigated. The ordered mesoporous carbon based solid-contact Ag^+-ISE shows a linear potential response in the range of 1.0×10^{-6}-1.0×10^{-3} M $AgNO_3$ with the slope of 55.6 ± 0.8 mV/dec (n=7) and the detection limit of $10^{-6.8}$ M. Additionally, the proposed solid-contact Ag^+-ISE is used to investigate the spontaneous dissolution of Ag NPs in deionized water and the stimulated dissolution of Ag NPs upon the addition of H_2O_2, separately. The obtained

results were validated by ICP-MS. This work shows that solid-contact Ag^+-ISEs provide a fast tool for real-time monitoring of the dissolution of Ag NPs released into the environment *e.g.* through wastewater.

Acknowledgements

T. J. Yin gratefully acknowledges the Johan Gadolin Scholarship provided by the Johan Gadolin Process Chemistry Centre at Åbo Akademi University and the financial support of the National Natural Science Foundation of China (41706110). This research is part of the activities of the Johan Gadolin Process Chemistry Centre, a centre of excellence at Åbo Akademi University.

References

[1] N. Lewinski, V. Colvin, R. Drezek, Cytotoxicity of nanoparticles, Small 4 (2008) 26-49.

[2] C. Marambio-Jones, E.M.V. Hoek, A review of the antibacterial effects of silver nanomaterials and potential implications for human health and the environment, J. Nanopart. Res. 12 (2010) 1531-1551.

[3] S. Kittler, C. Greulich, J. Diendorf, M. Köller, M. Epple, Toxicity of silver nanoparticles increases during storage because of slow dissolution under release of silver ions, Chem. Mater. 22 (2010) 4548-4554.

[4] C. Levard, E.M. Hotze, G.V. Lowry, G.E. Brown, Environmental transformations of silver nanoparticles: impact on stability and toxicity, Environ. Sci. Technol. 46 (2012) 6900-6914.

[5] C. Beer, R. Foldbjerg, Y. Hayashi, D.S. Sutherland, H. Autrup, Toxicity of silver nanoparticles-nanoparticle or silver ion?, Toxicol. Lett. 208 (2012) 286-292.

[6] C. Levard, B.C. Reinsch, F.M. Michel, C. Oumahi, G.V. Lowry, G.E. Brown, Sulfidation processes of pvp-coated silver nanoparticles in aqueous solution: impact on dissolution rate, Environ. Sci. Technol. 45 (2011) 5260-5266.

[7] M.A. Maurer-Jones, M.P.S. Mousavi, L.D. Chen, P. Bühlmann, C.L. Haynes, Characterization of silver ion dissolution from silver nanoparticles using fluorous-phase ion-selective electrodes and assessment of resultant toxicity to Shewanella oneidensis, Chem. Sci. 4 (2013) 2564-2572.

[8] B.S. Zhao, M. He, B.B. Chen, B. Hu, Ligand-assisted magnetic solid phase

extraction for fast speciation of silver nanoparticles and silver ions in environmental water, Talanta 183 (2018) 268-275.

[9] L.J. Dong, X.X. Zhou, L.G. Hu, Y.G. Yin, J.F. Liu, Simultaneous size characterization and mass quantification of the in vivo core-biocorona structure and dissolved species of silver nanoparticles, J. Environ. Sci. 63 (2018) 227-235.

[10] G.A. Sotiriou, A. Meyer, J.T.N. Knijnenburg, S. Panke, S.E. Pratsinis, Quantifying the origin of released Ag^+ ions from nanosilver, Langmuir 28 (2012) 15929-15936.

[11] O. Choi, K.K. Deng, N.-J. Kim, L. Ross, R.Y. Surampalli, Z. Hu, The inhibitory effects of silver nanoparticles, silver ions, and silver chloride colloids on microbial growth, Water Res. 42 (2008) 3066-3074.

[12] M. Koch, S. Kiefer, C. Cavelius, A. Kraegeloh, Use of a silver ion selective electrode to assess mechanisms responsible for biological effects of silver nanoparticles, J. Nanopart. Res. 14 (2012) 646-656.

[13] N.D. Fletcher, H.C. Lieb, K.M. Mullaugh, Stability of silver nanoparticle sulfidation products, Sci. Total Environ. 648 (2019) 854-860.

[14] J. Liu, F. Zhang, A.J. Allen, A.C. Johnston-Peck, J.M. Pettibone, Comparing sulfidation kinetics of silver nanoparticles in simulated media using direct and indirect measurement methods, Nanoscale 10 (2018) 22270-22279.

[15] M.P.S. Mousavi, I.L. Gunsolus, C.E. Pérez De Jesús, M. Lancaster, K. Hussein, C.L. Haynes, P. Bühlmann, Dynamic silver speciation as studied with fluorous-phase ion-selective electrodes: effect of natural organic matter on the toxicity and speciation of silver, Sci. Total Environ. 537 (2015) 453-461.

[16] C.Z. Lai, M.A. Fierke, R.C. da Costa, J.A. Gladysz, A. Stein, P. Buhlmann, Highly selective detection of silver in the low ppt range with ion-selective electrodes based on ionophore-doped fluorous membranes, Anal. Chem. 82 (2010) 7634-7640.

[17] J. Zhang, J.W. Ding, T.J. Yin, X.F. Hu, S.Y. Yu, W. Qin, Synthesis and characterization of monoazathiacrown ethers as ionophores for polymeric membrane silver-selective electrodes, Talanta 81 (2010) 1056-1062.

[18] E. Bakker, Electroanalysis with membrane electrodes and liquid–liquid interfaces, Anal. Chem. 88 (2016) 395-413.

[19] J. Bobacka, A. Ivaska, A. Lewenstam, Potentiometric ion sensors, Chem. Rev. 108 (2008) 329-351.

[20] C.-Z. Lai, M.A. Fierke, A. Stein, P. Bühlmann, Ion-selective electrodes with three-dimensionally ordered macroporous carbon as the solid contact, Anal. Chem. 79 (2007) 4621-4626.

[21] C.Z. Lai, M.M. Joyer, M.A. Fierke, N.D. Petkovich, A. Stein, P. Buhlmann, Subnanomolar detection limit application of ion-selective electrodes with three-dimensionally ordered macroporous (3DOM) carbon solid contacts, J. Solid State Electrochem. 13 (2009) 123-128.

[22] J.B. Hu, X.U. Zou, A. Stein, P. Buhlmann, Ion-selective electrodes with colloid-imprinted mesoporous carbon as solid contact, Anal. Chem. 86 (2014) 7111-7118.

[23] J.H. Li, T.J. Yin, W. Qin, An effective solid contact for an all-solid-state polymeric membrane Cd^{2+}-selective electrode: Three-dimensional porous graphene-mesoporous platinum nanoparticle composite, Sens. Actuators B 239 (2017) 438-446.

[24] T. Yin, D. Pan, W. Qin, All-solid-state polymeric membrane ion-selective miniaturized electrodes based on a nanoporous gold film as solid contact, Anal. Chem. 86 (2014) 11038-11044.

[25] R.I. MacCuspie, Colloidal stability of silver nanoparticles in biologically relevant conditions, J. Nanopart. Res. 13 (2011) 2893-2908.

[26] P.K. Tripathi, L.H. Gan, M.X. Liu, N.N. Rao, Mesoporous carbon nanomaterials as environmental adsorbents, J. Nanosci. Nanotechnol. 14 (2014) 1823-1837.

[27] M.-J. Deng, C.-C. Wang, P.-J. Ho, C.-M. Lin, J.-M. Chen, K.-T. Lu, Facile electrochemical synthesis of 3D nano-architectured CuO electrodes for high-performance supercapacitors, J. Mater. Chem. A 2 (2014) 12857-12865.

[28] J. Bobacka, Potential stability of all-solid-state ion-selective electrodes using conducting polymers as ion-to-electron transducers, Anal. Chem. 71 (1999) 4932-4937.

[29] K. Wygladacz, A. Radu, C. Xu, Y. Qin, E. Bakker, Fiber-optic microsensor array based on fluorescent bulk optode microspheres for the trace analysis of silver ions, Anal. Chem. 77 (2005) 4706-4712.

[30] T.J. Yin, Y.Y. Liu, W. Qin, Single-piece solid-contact polymeric membrane ion-selective electrodes for silver ion, J. Electrochem. Soc. 160 (2013) B91-B94.

[31] T. Lindfors, J. Szuecs, F. Sundfors, R.E. Gyurcsanyi, Polyaniline nanoparticle-based solid-contact silicone rubber ion-selective electrodes for ultratrace measurements, Anal. Chem. 82 (2010) 9425-9432.

[32] J.H. On, K.T. Cho, Y. Park, S. Hahm, W. Kim, J.Y. Cho, J.H. Hwang, Y.M. Jun, G.S. Cha, H. Nam, B.H. Kim, Synthesis of 7-deoxycholic amides or cholanes

containing distinctive ion-recognizing groups at C3 and C12 and evaluation for ion-selective ionophores, Tetrahedron 65 (2009) 1415-1423.

[33] J. Zhang, J. Ding, T. Yin, X. Hu, S. Yu, W. Qin, Synthesis and characterization of monoazathiacrown ethers as ionophores for polymeric membrane silver-selective electrodes, Talanta 81 (2010) 1056-1062.

[34] D. Paramelle, A. Sadovoy, S. Gorelik, P. Free, J. Hobley, D.G. Fernig, A rapid method to estimate the concentration of citrate capped silver nanoparticles from UV-visible light spectra, Analyst 139 (2014) 4855-4861.

[35] B.J. Marquis, M.A. Maurer-Jones, K.L. Braun, C.L. Haynes, Amperometric assessment of functional changes in nanoparticle-exposed immune cells: varying Au nanoparticle exposure time and concentration, Analyst 134 (2009) 2293-2300.

[36] F. Gottschalk, T. Sonderer, R.W. Scholz, B. Nowack, Modeled environmental concentrations of engineered nanomaterials (TiO_2, ZnO, Ag, CNT, Fullerenes) for different regions, Environ. Sci. Technol. 43 (2009) 9216-9222.

[37] S.A. Blaser, M. Scheringer, M. MacLeod, K. Hungerbühler, Estimation of cumulative aquatic exposure and risk due to silver: contribution of nano-functionalized plastics and textiles, Sci. Total Environ. 390 (2008) 396-409.

Figure captions

Fig. 1 Cyclic voltammograms recorded in 0.1 M KNO_3 for the bare GC electrode, and ordered mesoporous carbon and disordered mesoporous carbon modified GC electrodes. Scan rate = 100 mV/s. Inset: SEM images of the ordered mesoporous carbon and disordered mesoporous carbon materials.

Fig. 2 Impedance spectra for the ordered mesoporous carbon and the disordered mesoporous carbon modified GC electrodes in 0.1 M KNO_3. Frequency range = 0.01 Hz to 100 kHz; E_{dc} = open circuit potential; $\triangle E_{ac}$ = 10 mV. Inset: magnification of the impedance spectra in the frequency range from 0.1 Hz to 100 kHz.

Fig. 3 Multi-chronopotentiograms for the bare GC electrode (dash-dot line), and ordered mesoporous carbon (solid line) and disordered mesoporous carbon (dash line) modified GC electrodes in 0.1 M KNO_3. Applied current = +1 nA for 60 s and -1 nA for 60 s (5 cycles).

Fig. 4 Calibration curve for the ordered mesoporous carbon-based solid-contact Ag^+-selective electrode. Error bars represent the standard deviation for seven identical electrodes. Inset: time-dependent potential response trace for the proposed electrode.

Fig. 5 Potential stability of the ordered mesoporous carbon-based solid-contact Ag^+-selective electrode recorded in 1.0×10^{-5} and 1.0×10^{-4} M $AgNO_3$ for 16 h. Solid line: the raw potential response of the electrode; dotted line: the linear fit of the raw data used for calculating the potential drifts.

Fig. 6 Characterization of the citrate-capped silver nanoparticles, including TEM images (a), histogram of Ag NPs sizes (b), typical UV-visible spectrum of the prepared

Ag NP solution.

Fig. 7 Characterization of the spontaneous dissolution of Ag NPs in deionized water，including the real-time potential response of the ordered mesoporous carbon-based solid-contact Ag^+-selective electrode upon the addition of silver nanoparticle solution in deionized water (a), and the real-time concentration changes of Ag^+ as calculated from the calibration curve in Fig. 4 (b). The discrete points are obtained by ICP-MS through collecting the supernatants of Ag NP solution at 1, 2, 4, 6 and 8 h. Error bars represent the standard deviations obtained from three measurements for ICP-MS and six measurements for the proposed Ag^+-selective electrode, respectively.

Fig. 8 Real-time potentiometric monitoring of the stimulated dissolution of Ag NPs in deionized water by using the ordered mesoporous carbon-based solid-contact Ag^+-selective electrode upon the addition of 1.0×10^{-5} and 2.0×10^{-5} M H_2O_2 in the Ag NP solution (a), and the real-time concentration changes of Ag^+ as calculated from the calibration curve in Fig. 4 (b).

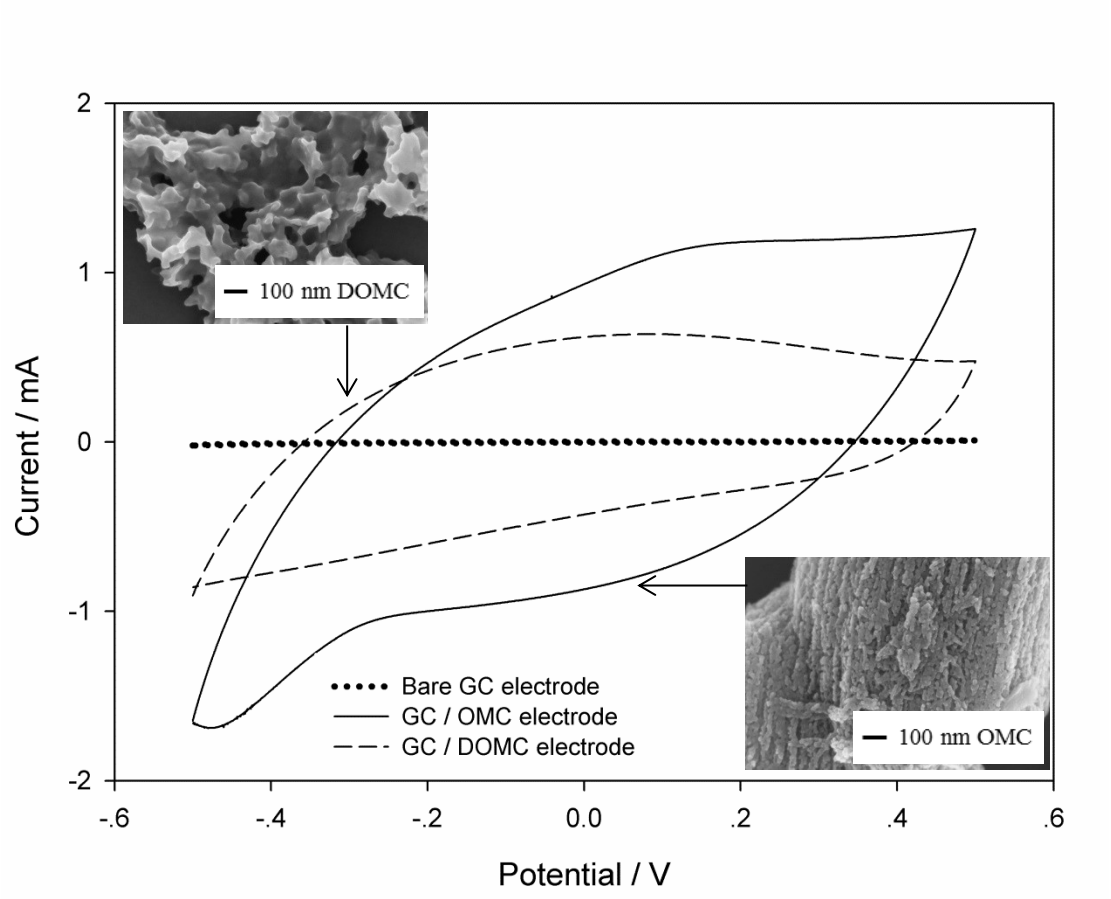
2
1
0
-1
-2
Current / mA
-.6
-.4
-.2
0.0
.2
.4
.6
Potential / V
100 nm DOMC
100 nm OMC
Bare GC electrode
GC / OMC electrode
GC / DOMC electrode

Fig. 1

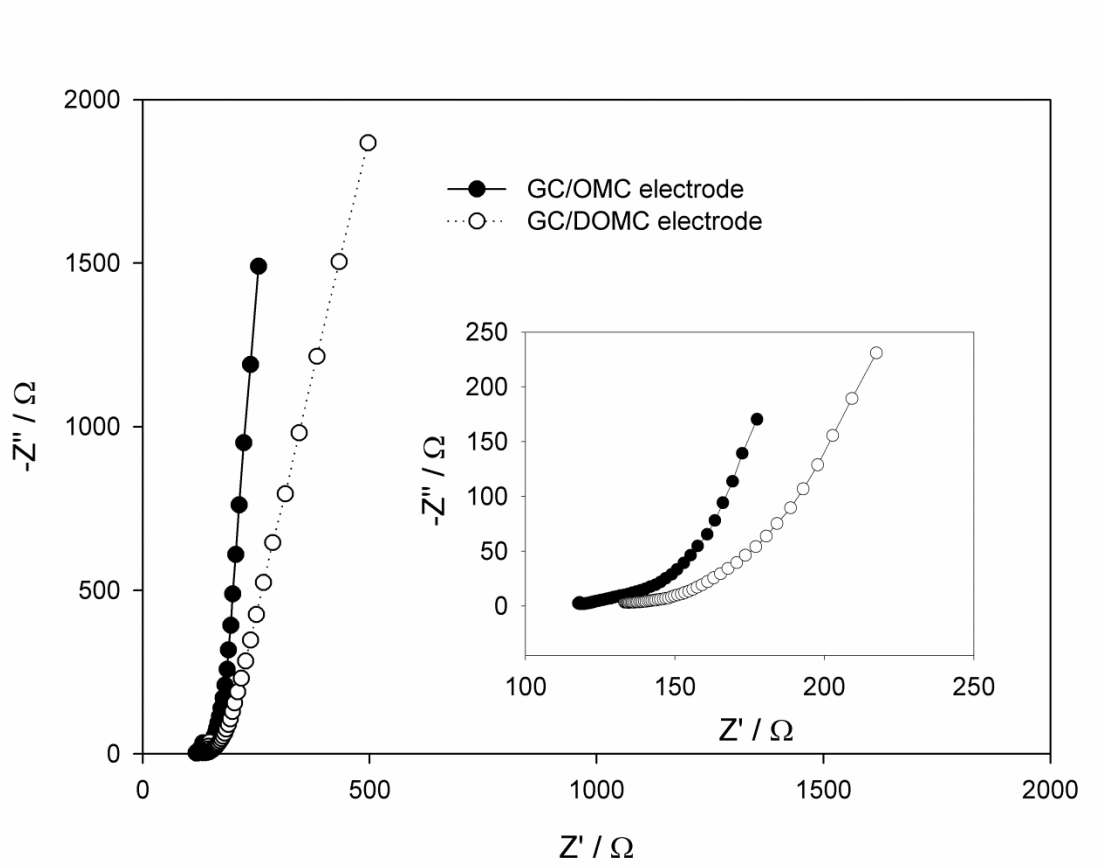
GC/OMC electrode
GC/DOMC electrode
-Z'' / Ω
Z' / Ω
0
500
1000
1500
2000
100
150
200
250
50

Fig. 2

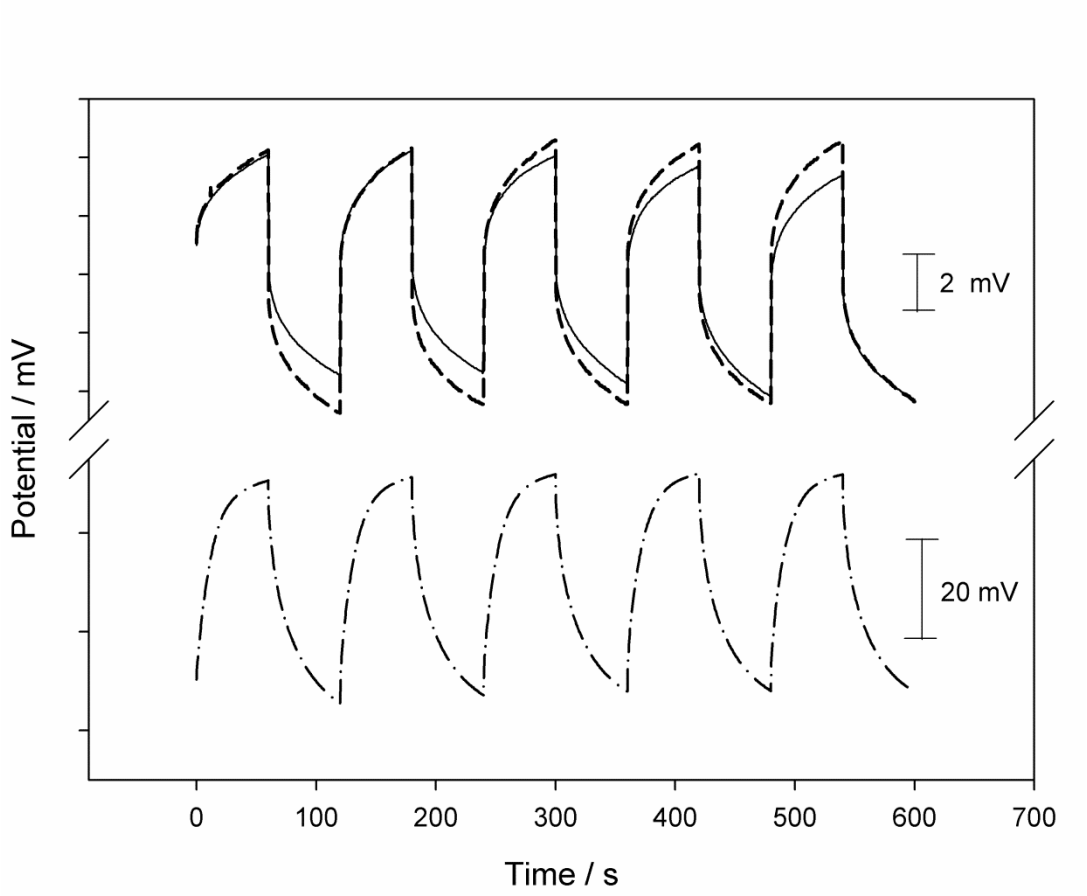

Fig. 3

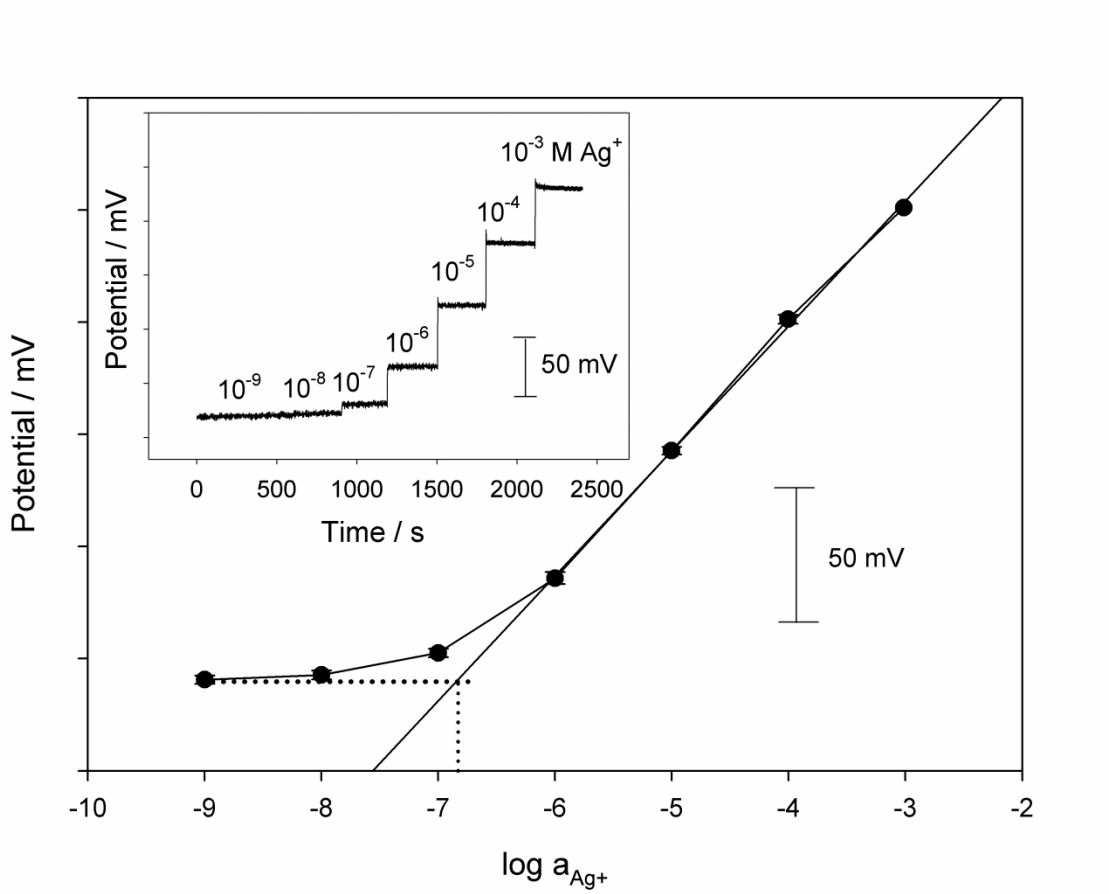
Potential / mV
log a$_{Ag+}$
-10
-9
-8
-7
-6
-5
-4
-3
-2
50 mV
Potential / mV
Time / s
0
500
1000
1500
2000
2500
10^{-9}
10^{-8}
10^{-7}
10^{-6}
10^{-5}
10^{-4}
10^{-3} M Ag^{+}
50 mV

Fig. 4

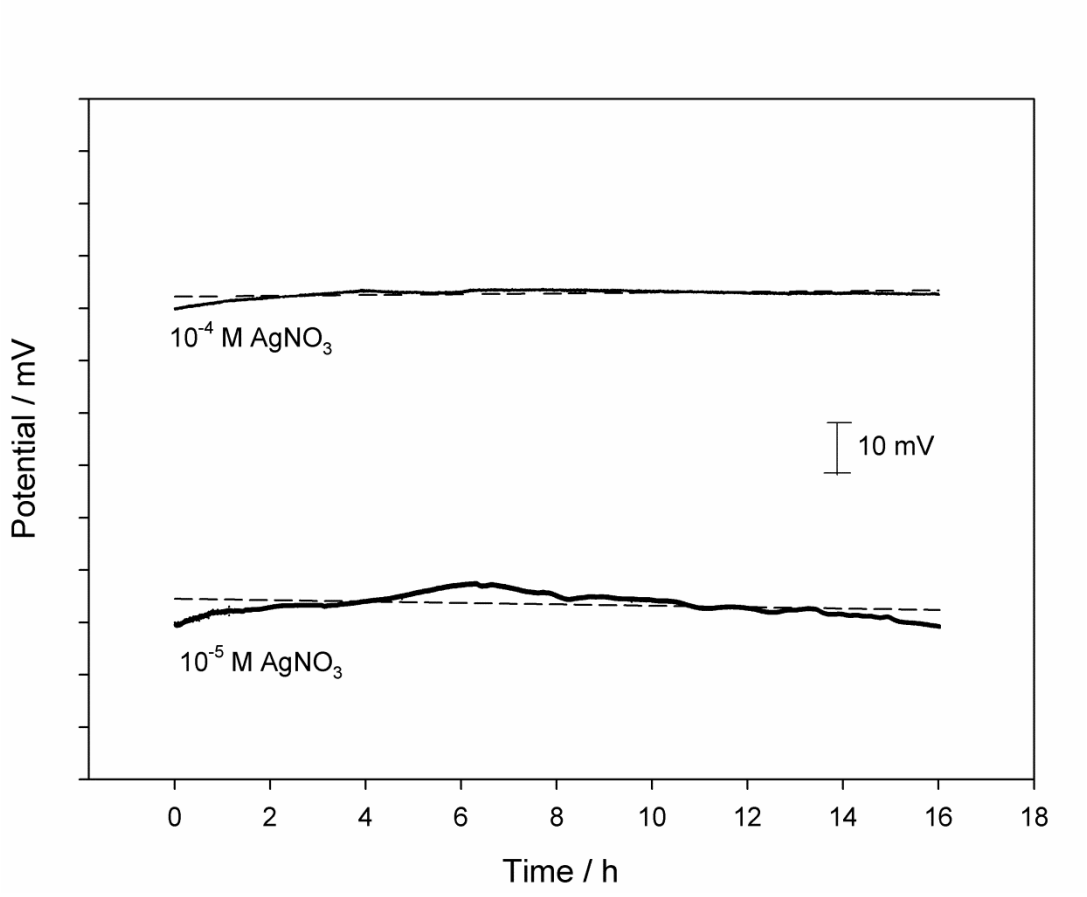
Potential / mV
10^{-4} M $AgNO_3$
10 mV
10^{-5} M $AgNO_3$
0
2
4
6
8
10
12
14
16
18
Time / h

Fig. 5

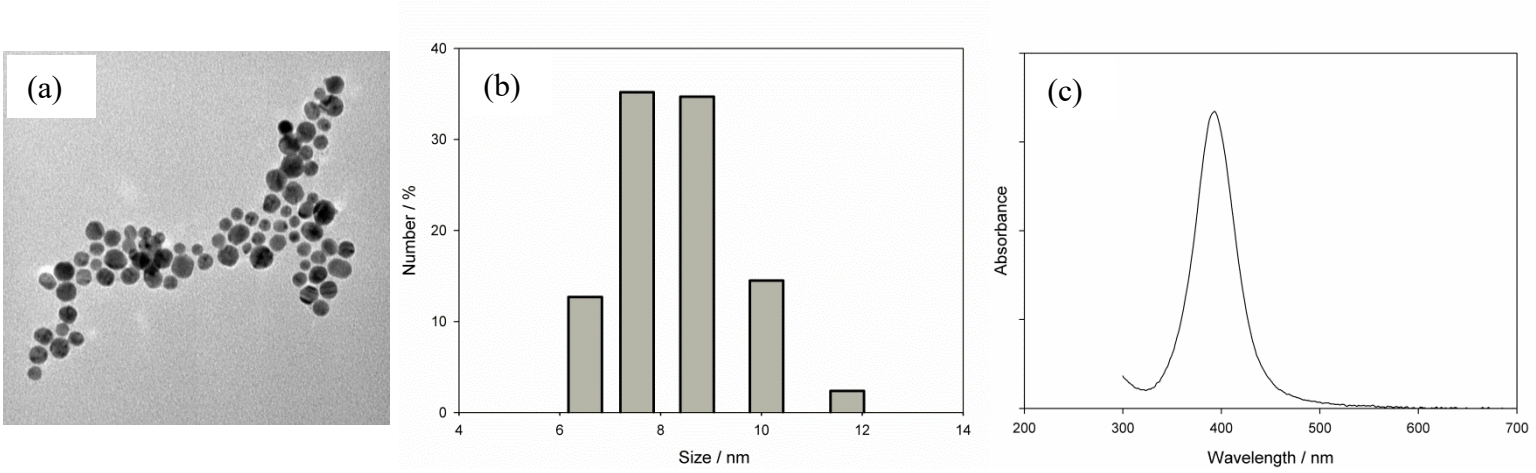

Fig. 6

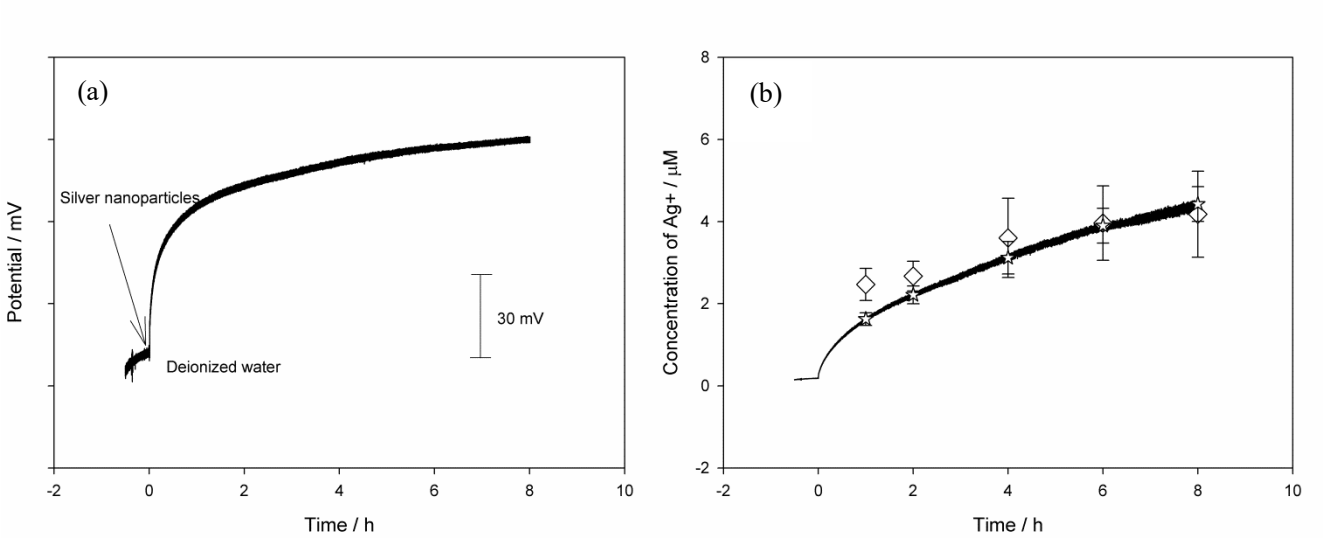
(a)
Silver nanoparticles
Deionized water
30 mV
Potential / mV
Time / h
(b)
Concentration of Ag+ / μM
Time / h

Fig. 7

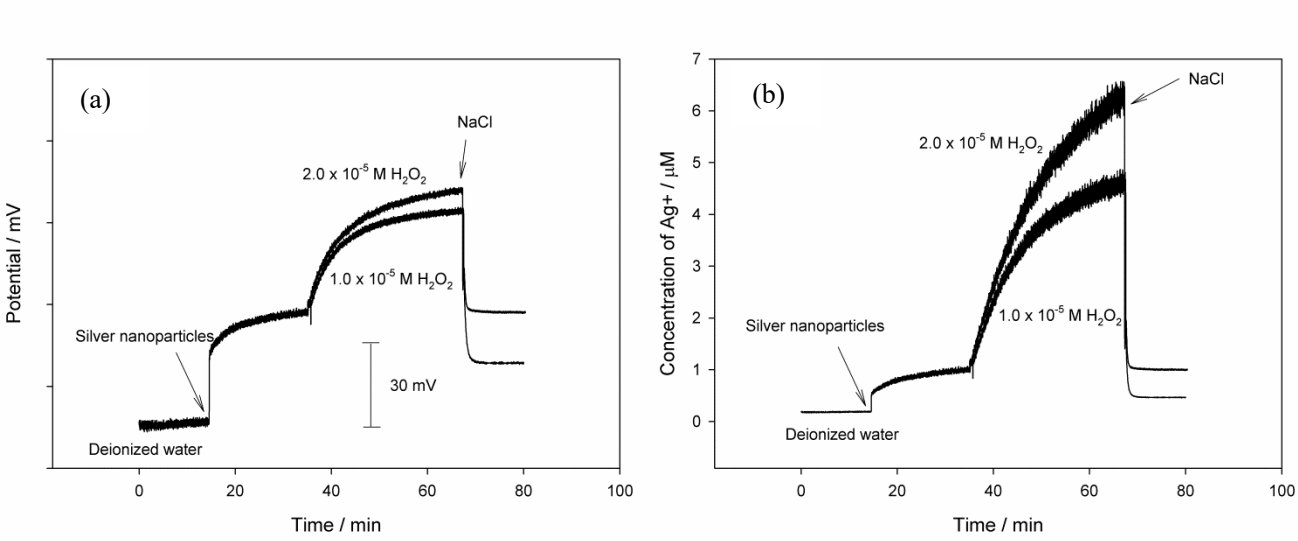
(a)
NaCl
2.0 x 10-5 M H2O2
1.0 x 10-5 M H2O2
Silver nanoparticles
30 mV
Deionized water
Potential / mV
Time / min
(b)
NaCl
2.0 x 10-5 M H2O2
1.0 x 10-5 M H2O2
Silver nanoparticles
Deionized water
Concentration of Ag+ / μM
Time / min

Fig. 8

TOC graphic

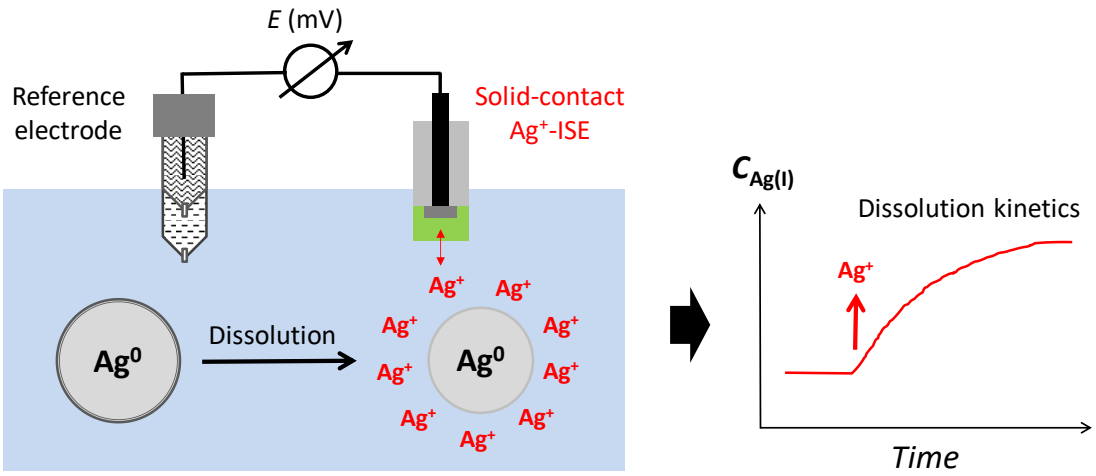
E (mV)
Reference electrode
Solid-contact Ag+-ISE
Ag+
Ag+
Ag+
Ag+
Ag+
Ag+
Ag+
Ag+
Ag0
Dissolution
Ag0
C Ag(I)
Dissolution kinetics
Ag+
Time

Highlights

1. A mesoporous carbon-based solid-contact Ag^+-selective electrode is constructed.
2. The solid-contact Ag^+-selective electrode shows a good potential stability.
3. The solid-contact Ag^+ selective electrode shows a detection limit of $10^{-6.8}$ M.
4. Spontaneous and stimulated dissolution of Ag NPs to Ag^+ is monitored in real time.
5. Results validated by ICP-MS.